Research Article: Open Access

VIBGYOR ePress

International Journal of
Nanoparticles and Nanotechnology

Sound Absorption and Transmission in Nanoengineered Polymers

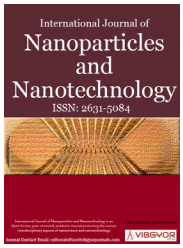

ISSN: 2631-5084

Wasim A Orfali*

Architectural Engineering Department, College of Engineering, Taibah University, Saudi Arabia

Abstract

In this study we use vapor deposition to incorporate carbon nanotubes (CNTs) and silicon dioxide nanopowder (nanosilica) in Polyurethane (PU) as well as to engineer Parylene C (PC) in a microfibrous thin film (μFTF) and bulk forms in an attempt to examine acoustic absorption and transmission properties in the low frequency (50 to 200 Hz) range. Incorporating CNTs or/and nanosilica into PU significantly increases its acoustic transmission, presumably due to increased rigidity caused by nanoparticle (CNTs and nanosilica) addition. This is explained as due to adding nanosilica or/and CNTs to PU increases its rigidity and, hence, its sound transmission. On the other hand, engineering the PC in the μFTF form enhances acoustic absorption in the film, especially at the resonant frequencies associated with oscillations of the microfibers making up the PC μFTF.

Introduction

Parylene C (PC), a polymer material with molecular form -$(C_8H_7Cl)_n$-, was first developed in 1947 [1]. It has been in use as protective insulation-coatings in medical devices and electronic appliances as well as substrates for the growth and proliferation of biological cells [2-4]. Moreover, PC is widely used as a moisture-barrier coating on implantable devices such as stents, defibrillators, and pacemakers [5-8]. PC films are also used as gas-sensing membranes in microelectromechanical systems [9].

Polyurethane (PU) is another polymer, which finds a number of uses in everyday life and applications. It is composed of organic units joined by urethane [-NH-(C=O)-O] links [10]. PU foams have cellular structure, which improves sound absorbing and insulating properties [11]. A number of studies have been undertaken to examine the use of nanoclay [12], titania nanoparticles [13,14] carbon nanotubes (CNTs) reinforced PU to modulate its sound absorption properties.

Microfibrous thin films (μFTFs) are important materials in optical, chemical and biochemical applications [4,15,16]. μFTFs are fabricated by either physical or chemical vapor deposition methods with oblique-angle deposition techniques [17]. Different material types, including metals, ceramics and polymers have been successfully sculptured using these techniques. Also, nanoengineering polymers during synthesis are found to give them numerous properties that are attractive for applications in many areas ranging from electronics to

***Corresponding author:** *Wasim A Orfali, Architectural Engineering Department, College of Engineering, Taibah University, P.O. Box 344, Saudi Arabia*

Accepted: November 05, 2018; **Published:** November 07, 2018

Orfali. Int J Nanoparticles Nanotech 2018, 4:019

ISSN 2631-5084

9 772631 508002

Citation: Orfali WA (2018) Sound Absorption and Transmission in Nanoengineered Polymers. Int J Nanoparticles Nanotech 4:019

optoelectronics, microelectromechanical systems, and biomedical devices. Common methods of nanoengineering polymers involve the incorporation of nanoparticles and CNTs into the polymer material matrices.

In this work we examine PC and PU acoustic absorption and sound transmission as functions of film morphology and composition in the audible low frequency range. We find out that the porosity and structural periodicity increases absorption in the μFTFs in comparison with the dense PC films. The increase in absorption is observed to be about an order of magnitude at resonant frequencies. We also find that adding silicon oxide nanopowder (nanosilica) or/and CNTs to PU significantly changes its sound transmission characteristics.

Experimental Procedure

The columnar μFTFs of PC were grown on p-type Si substrates using oblique angle physicochemical vapor deposition in the same PDS2010 Labcoater described above. Four grams of commercial PC dimer was first vaporized at 175 °C and then pyrolyzed into reactive monomers at 690 °C. The vapor of reactive monomers was collimated using a nozzle and directed onto 20 mm (length) × 20 mm (breadth) substrate, where room-temperature polymerization of the reactive monomers took place. The low-pressure chamber was maintained at 175 °C and 28 mTorr. The incidence angle of the collimated flux with respect to the substrate plane was set equal to 45°. The columnar μFTF thickness was controlled by adjusting the amount of PC dimer evaporated, and was found to be ~100 μm, as measured by P-16+ a KLA-Tencor profilometer. The deposition of the bulk PC films was done at set pressure of 28 mTorr, furnace at temperature 690 °C, and vaporizer at 175 °C. Unlike the μFTF deposition the bulk PC deposition was done using vertical vapor incidence on the p-type Si substrate. By adjusting the evaporated dimer mass, bulk PC films of thicknesses of ~10 microns were grown on the Si substrate. Each microfibrous or bulk PC thin film was removed from the silicon substrate using a razor.

In addition to examining bulk and fibrous polymer acoustic absorption, the effects on sound transmission of incorporating CNTs and nanoparticles into polymers was one other main objective of this work. Hence, CNTs and nanosilica were added to the polyol and isocyanate composition to control sound transmission and absorption in PU. PU foam mixtures were prepared at different weight ratios (0.2%, 0.5%, 1%) of silica nano-powder, different weight ratios (0.35%, 0.7%, 2%) of CNTs, or silica nano-powder (0.5% weight ratio) plus (1% weight ratio) CNTs.

After removal, each PC μFTF sample was held between the two grips (10.85 mm apart for one sample, 7.8 mm for the other) of a tension clamp and subjected to cyclic loading in a Model Q800 Dynamic Mechanical Analyzer (DMA) using the 'Multi-Frequency Strain module. The DMA was manufactured by TA Instruments, Newcastle, DE, U.S.A. The tension-clamp was calibrated with a thin steel sheet of known compliance and dimensions. A cyclic strain of amplitude 0.046% (elastic regime) was set for frequencies between 5 and 200 Hz with an increment of 5 Hz.

The bulk PC and the PU films' transmission loss data were generated in a Bruel & Kjaer impedance tube. The films were inserted into the tube. A loudspeaker in the tube emits precisely quantified sound, and the microphones measure the sound pressure level at specific locations along the length of the tube. Commercial software was then used to extract normal incidence acoustic properties as functions of frequency.

The morphologies of the films were examined using a field-emission scanning electron microcopy (FESEM) utilizing Model LEO 1530, Carl Zeiss, microscope.

Results and Discussion

Effects of polymer nano-composition

Figure 1 contrasts transmission loss (TL) results for pure PU and PU treated with nanosilica at a 0.2% weight ratio, or CNTs at a weight ratio of 035%. TL is defined as

$$TL = 10Log_{10}\left|\frac{I_i}{I_t}\right| \quad (1)$$

Where I_i and I_t are the incident and transmitted sound intensities, respectively. TL is measured in decibels (db) as given in Figure 1 and the following figures.

Lower TL, which decreases with frequency in this range, was observed in PU containing the silica nanoparticles. It was observed that changing the silica nanoparticle weight ratio in PU did not significantly change TL. Figure 1 also shows the ef-

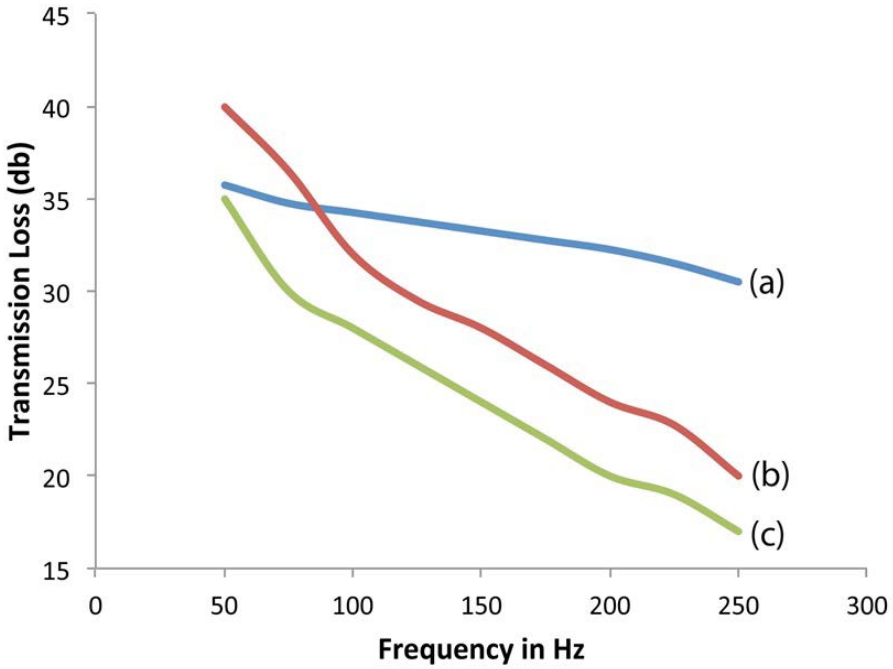

Figure 1: TL results a) In pure PU; b) In PU including 0.2% weight ratio of silica nano-powder; c) In PU including 0.35% weight ratio of CNTs.

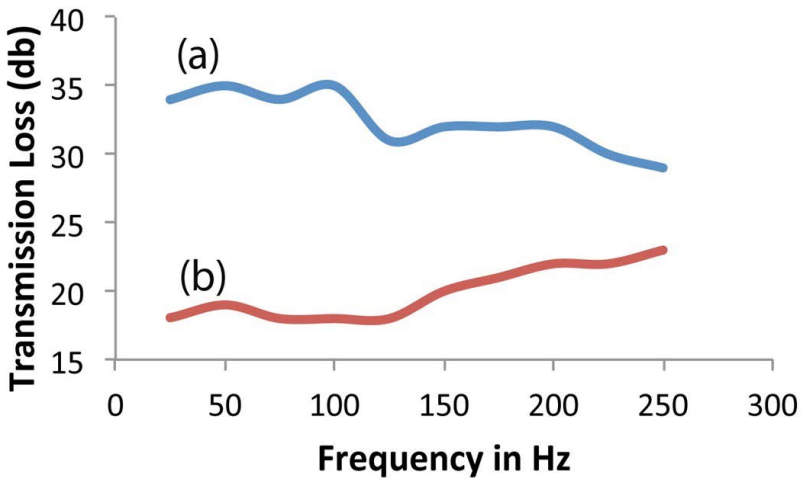

Figure 2: TL measured in a) Pure PU; b) In PU incorporating silica nano-powder at a 0.5% weight ratio and 1% weight ratio of CNTs.

fects on TL of adding CNTs to the composition of PU. Addition of CNTs at a weight ratio of 0.35% to PU decreased TL in the film, and TL decreased with frequency. The change produced by the CNT addition to PU was observed to be higher than that produced by the addition of the silica nano-powder and this change in TL was not much affected by varying the content of CNTs or nano-powder in the weight ratio up to 2%. The decrease of TL with frequency is also observed in pure TU films however to a lesser degree than that in films containing nanosilica and CNTs.

Figure 2 presents TL in films that incorporated both silica nano-powder and CNTs at weight ratios of 0.5% and 1%, respectively. It is seen from the results in Figure 2 that more change in TL of pure PU is caused by the addition of both CNTs and silica nano-powder. This conclusion is more evident in the results included in Figure 3, where the percentage change in TL is plotted for PU incorporating silica nano-powder, CNTs, or silica nano-powder plus CNTs. The percentage change in the latter films is observed to be more pronounced in most of the audible low-frequency range investigated.

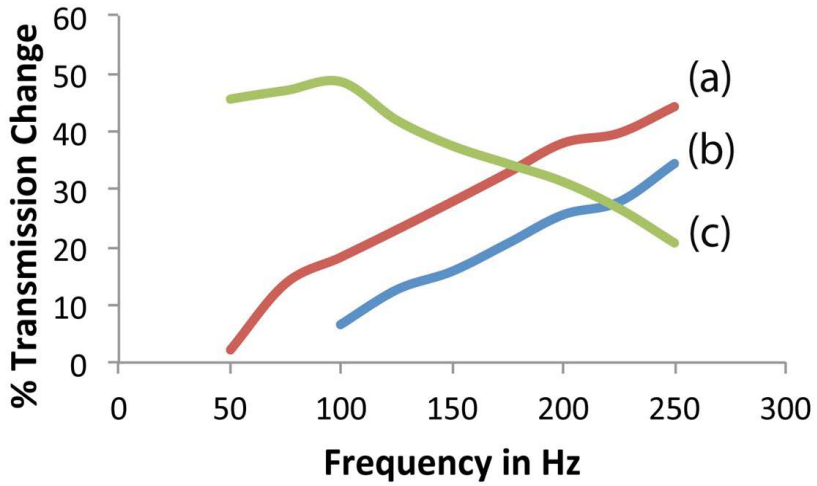

Figure 3: Percentage change in TL measured in a) In PU including 0.2% weight ratio of silica nano-powder; b) In PU including 0.35% weight ration of CNTs; and c) In PU incorporating silica nano-powder at a 0.5% weight ratio and 1% weight ratio of CNTs.

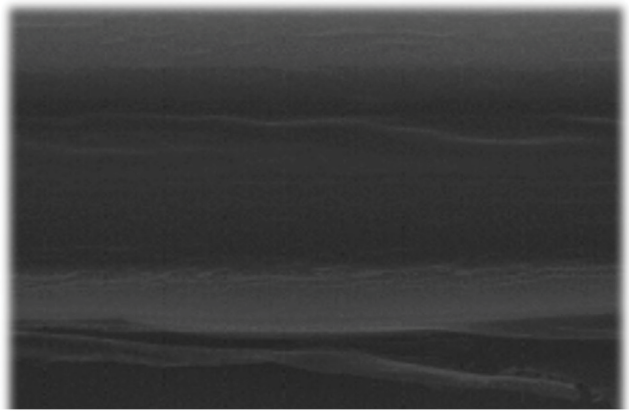

(a)

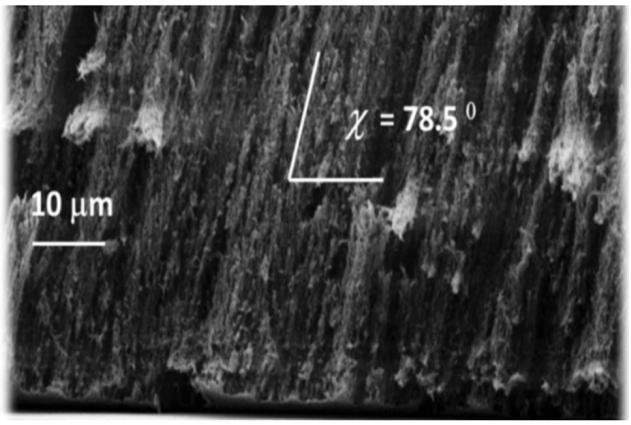

(b)

Figure 4: FESEM images taken in a) The bulk (dense) PC film [21]; b) In the PC µFTF film.

It has been previously reported that incorporating CNTs and nanoparticles in material composition increases its Young's modulus, *E*, and, hence, its rigidity [18-20]. Assuming that the material density, ρ, is not significantly affected by the incorporation of CNTs and nanoparticles, the increase in rigidity increases the speed of sound, *c*, in the material according to the relation $c \alpha \sqrt{\frac{E}{\rho}}$. The higher sound speed enhances sound propagation in the polymer and, hence, gives rise to a reduced transmission loss. This explains our observation that sound transmission increased in our PU films containing nanosilica and CNTs.

Effects of polymer morphology: Bulk versus microfibrous PC

Typical cross-sectional FESEM images in the xz plane of the PC films are shown in Figure 4. Figure 4a shows the dense bulk film whereas Figure 4b shows an image for the µFTF film. The columnar microfibers of cross-sectional diameter ~5 µm are tilted at ~78° in the xz plane, which is the morphologically significant plane of the columnar µFTF.

Figure 4 shows the significantly high porosity in the µFTF when contrasted with the bulk (dense form) PC, which is effectively free from pores. Given this high porosity in the µFTFs one expects the acoustic properties of Parylene C to be impacted as its growth method is varied. Therefore, in the results presented and discussed below the acoustic absorption coefficient in Parylene C is compared in dense and µFTF forms. The objective is to determine the range of the absorption coefficient, α, of PC, depending on its growth method, in order to explore its acoustic applications.

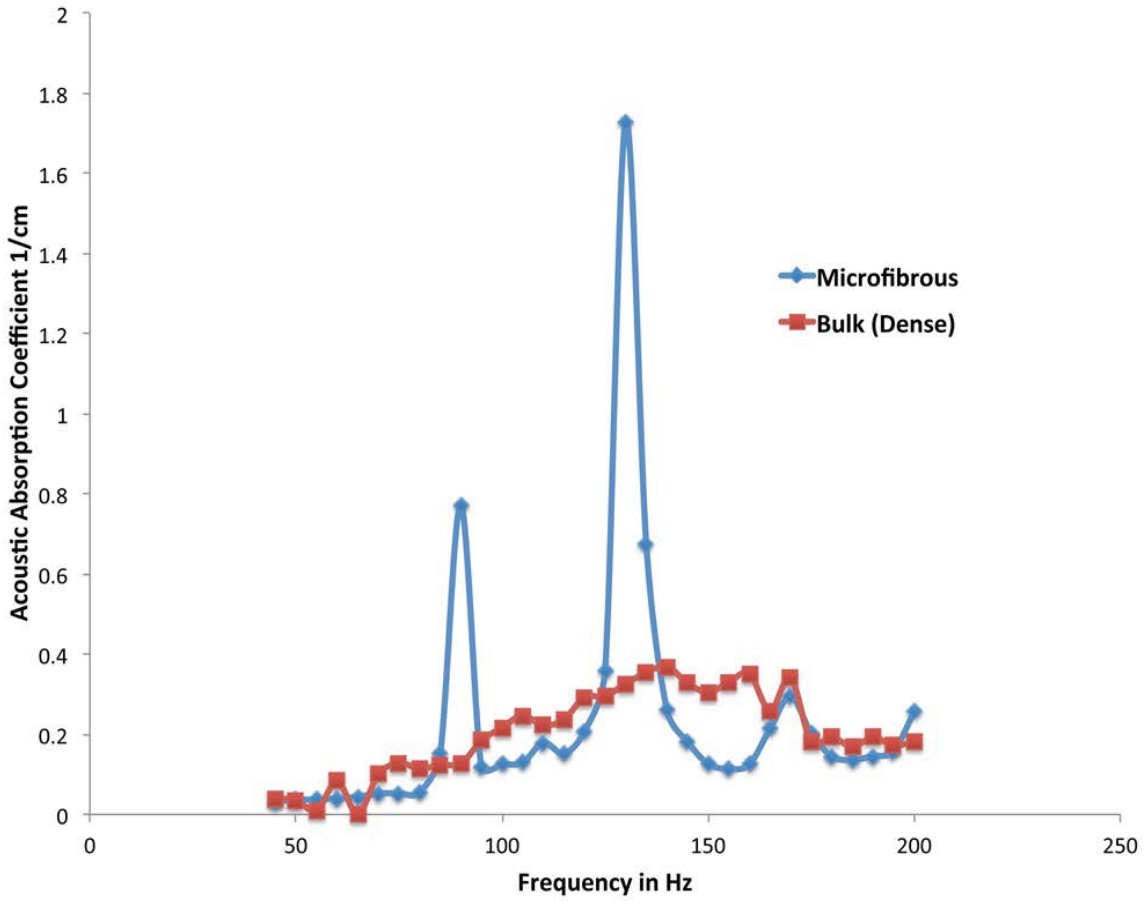

Figure 5: The acoustic absorption coefficient in a PC bulk and microfibrous films.

The acoustic absorption coefficient, α, determines the acoustic signal intensity, $I_t(x)$, as a function of the penetrated depth x into the film according to

$$I_t(x) = I_i e^{\alpha x} \quad (1)$$

Where I_i is the incident intensity.

Figure 5 shows the absorption coefficient in bulk PC films in the audible low-frequency range. These absorption coefficients were found to be strongly dependent on frequency and may attain values in the range 0.05 to 0.4 cm^{-1}. These values are within the ranges reported for polymers used in different acoustic applications [22]. α is observed to slightly vary with f and attains its highest values at ~130 Hz.

α for the PC µFTFs were determined from the dynamic loading measurements. For a linear material subjected to cyclic loading at frequency f a phase shift δ exists between stress σ and strain, which are given by

$$\sigma = \sigma_o \sin(\omega t) \text{ and } \in = \in_o \sin(\omega t + \delta) \quad (2)$$

Where t is time, σ_o and ε_o are the respective amplitudes of stress and strain, $\omega = 2\pi f$ is the angular frequency, and δ is a phase shift. The two elastodynamic moduli are the storage (elastic) modulus $E^1 = \frac{\sigma_o}{\varepsilon_o}\cos\delta$ and the loss modulus $E^{11} = \frac{\sigma_o}{\varepsilon_o}\sin\delta$ [23]. The absorption coefficient, α, is obtained from the phase shift δ using the relation.

$$\alpha = \frac{\omega}{2c} tan\delta \text{ where } c = \sqrt{\frac{E^1}{\rho}} \quad (3)$$

Where ρ is the film density.

Figure 5 also presents α in the PC µFTF and compares it to the acoustic absorption data in the bulk film. In the acoustic frequency range 50 to 200 Hz, one observes that α values are comparable except for three remarkably distinct peaks in α observed in the PC µFTFs. The peak values of α at ~90 Hz and ~125 Hz, 0.8 and 1.7, respectively, are significantly higher than α in bulk PC by almost an order of magnitude. The third peak at ~170 Hz comes with a α value of ~0.3. It is also observed that these three peaks are very narrow in frequency with peak widths at half-α values of ~5 Hz. It is important to

note that α in the PC μFTFs is expected to be anisotropic because of the morphology anisotropy in the deposited film (Figure 2b). The acoustic absorption coefficient shown in Figure 5 is the on-plane component, which is transverse to the film columnar fibers. On the other hand, α in the bulk film is expected to be isotropic since the film morphology is homogeneous in the bulk film.

The highest peak in α at f~125 Hz is attributed to the resonant frequency of the vibrating microfibers in the PC μFTF, whereas the two remaining peaks are suggested to arise from secondary resonance frequencies, presumably arising from variations in μFTF morphology [24]. The results presented in Figure 5 clearly establish that PC μFTFs are much superior to bulk PC films in low-frequency sound isolation.

Conclusion

The effects of the addition small amount of CNTs and silica nano-powder into PU foam on the sound absorption were also investigated. The experiments showed that addition of up to 1% weight ratio silica nano-powder and up to 2% weight ratio of carbon nanotubes to polyurethane composition improved sound transmissions loss by up to 50% than that of pure polyurethane foam sample.

In this study PC bulk films and μFTFs were prepared and examined for their low frequency acoustic absorption properties. Both film types were grown using physicochemical vapor deposition. The μFTFs were grown using oblique angle vapor deposition enabled by a rotating substrate holder, whereas the bulk films were prepared using vertical vapor deposition onto the substrate. Prior to the acoustic absorption measurements, cross-sectional FESEM micrographs were taken in the films. The FESEM films revealed the columnar nature of the μFTFs and have shown the higher porosity in the μFTFs as compared to the bulk films.

The two PC types were examined for sound absorption by measuring the acoustic absorption coefficient. The absorption in the bulk films was measured using a type 4206 Bruel & Kjaer impedance tube, whereas the absorption results in the μFTFs were extracted from cyclic loading of the film in a DMA using the 'Multi-Frequency - Strain' module. In the audible low frequency acoustic range 50 to 200 Hz the absorption is comparable in the two film types, however the sound absorption in the μFTFs is significantly increased at the resonant frequencies of oscillations of the film microfibers.

References

1. JB Fortin, TM Lu (2004) Chemical vapor deposition polymerization: The growth and properties of parylene thin films. Kluwer Academic, Netherlands.
2. JP Seymour, YM Elkasabi, HY Chen, J Lahann, DR Kipke (2009) The insulation performance of reactive parylene films in implantable electronic devices. Biomaterials 30: 6158-6167.
3. GE Loeb, MJ Bak, M Salcman, EM Schmidt (1977) Parylene as a chronically stable, reproducible microelectrode insulator. IEEE Trans Biomed Eng 24: 121-128.
4. W Li, DC Rodger, E Meng, JD Weiland, MS Humayun, et al. (2010) Wafer-level parylene packaging with integrated RF electronics for wireless retinal prostheses. Journal of Microelectromechanical Systems 19: 735-742.
5. X Xie, L Rieth, L Williams, S Negi, R Bhandari, et al. (2010) Long-term reliability of Al_2O_3 and Parylene C bilayer encapsulated Utah electrode array based neural interfaces for chronic implantation. J Neural Eng 11: 026016.
6. S Takeuchi, D Ziegler, Y Yoshida, K Mabuchi, T Suzuki (2005) Parylene flexible neural probes integrated with microfluidic channels. Lab Chip 5: 519-523.
7. AB Fontaine, K Koelling, S Dos Passos, J Cearlock, R Hoffman, et al. (1996) Polymeric surface modifications of tantalum stents. J Endovasc Surg 3: 276-283.
8. T Trantidou, DJ Payne, V Tsiligkiridis, YC Chang, C Toumazou, et al. (2013) The dual role of Parylene C in chemical sensing: Acting as an encapsulant and as a sensing membrane for pH monitoring applications. Sensors and Actuators B: Chemical 186: 1-8.
9. T Xu, B Lu, YC Tai, A Goldkorn (2010) A cancer detection platform which measures telomerase activity from live circulating tumor cells captured on a microfilter. Cancer Res 70: 6420-6426.
10. E Delebecq, JP Pascault, B Boutevin, F Ganachaud, François (2013) On the versatility of urethane/urea bonds: Reversibility, blocked isocyanate, and non-isocyanate polyurethane. Chem Rev 113: 80-118.
11. http://www.eurofoam.hu/Application/technical-foam-department/audiotec-absorption/2/
12. X Cao, LJ Lee, T widya, C Macosko (2005) Polyurethane/clay nanocomposites foams: Processing, structure and properties. Polymer 46: 775-783.
13. H Mahfuz, VK Rangari, MS Islam, S Jeelani (2004) Fabrication, synthesis and mechanical characteriza-

tion of nanoparticles infused polyurethane foams. Composites Part A: Applied Science and Manufacturing 35: 453-460.

14. H Mahfuz, MS Islam, VK Rangari, MC Saha, S Jeelani (2004) Response of sandwich composites with nanophased cores under flexural loading. Composites Part B: Engineering 35: 543-550.
15. RR Søndergaard, M Hosel, FC Krebs (2012) Roll-to-roll fabrication of large area functional organic materials. Journal of Polymer Science Part B: Polymer Physics 51: 16-34.
16. YS Suzuki, Y Tai (2006) Micromachined high-aspect-ratio Parylene spring and its application to low-frequency accelerometers. Journal of Microelectromechanical Systems 15: 1364-1370.
17. WF Gorham (1996) A new, general synthetic method for the preparation of linear Poly-p-xylylenes. Journal of Polymer Science Part A-1: Polymer Chemistry 4: 3027-3039.
18. SJV Frankland, VM Harik, GM Odegard, DW Brenner, TS Gates (2003) The stress-strain behavior of polymer-nanotube composites from molecular dynamic simulation. Composites Science and Technology 63: 1655-1661.
19. R Zhu, E Pan, AK Roy (2007) Molecular dynamics study of the stress-strain behavior of carbon-nanotube reinforced Epon 862 composites. Materials Science and Engineering: A 447: 51-57.
20. B Arash, Q Wang, VK Varadan (2014) Mechanical properties of carbon nanotubes/polymer composites. Scientific Reports 4.
21. L Wei (2011) Fibrous parylene-C thin-film substrates for implant integration and protein assays. The Pennsylvania State University, USA.
22. L Yuvaraj, G Vijay, S Jeyanthi (2016) Study of sound absorption properties on rigid polyurethane foams using FEA. Indian Journal of Science and Technology 9.
23. Lakes R (1998) Viscoelastic Solids. CRC Press, Boca Raton, FL, USA.
24. Chadraprakash C, Lakhtakia A, Brown NR, Orfali W, Awadelkarim OO (2014) Frequency-and temperature-dependent storage and loss moduli of microfibrous thin films of Parylene C. Material Letters 116: 296-298.

ISSN 2631-5084